Electronic Supplementary Information

In-situ growth of α-Fe_2O_3@Co_3O_4 core-shell wormlike nanoarrays for highly efficient photoelectrochemical water oxidation reaction

Chenmei Li,[†,‡,‖] Zhihui Chen,[§,‖] Weiyong Yuan,*[,†,‡] Qing-Hua Xu,[§] and Chang Ming Li[†,‡]

[†]Institute for Clean energy & Advanced Materials, Faculty of Materials & Energy, Southwest University, Chongqing 400715, China.

[‡]Chongqing Key Laboratory for Advanced Materials and Technologies of Clean Energies, Chongqing 400715, China.

[§]Department of Chemistry, National University of Singapore, 3 Science Drive 3, Singapore 117543, Singapore

*Corresponding author. E-mail address: yuanweiyong@swu.edu.cn

‖These authors contributed equally.

Contents

1. Calculation of photoconversion efficiency

The photoconversion efficiency of a photoanode was calculated according to the following formula:[1-2]

$$\eta\% = \frac{J(1.23 - V)}{P} \times 100$$

Where J is the current density under simulated sunlight irradiation, V is the applied voltage versus RHE, and P is the light intensity (100 mW•cm^{-2}).

2. Calculation of flatband potential and donor density

The depletion layer capacitance obtained from the electrochemical impedance spectra can be described by the Mott−Schottky equation:[1, 3]

$$\frac{1}{C^2} = \frac{2}{e_0 \varepsilon \varepsilon_0 N_d}[(V - V_{FB}) - \frac{kT}{e_0}]$$

where e_0 is the electron charge, ε the dielectric constant of α-Fe_2O_3, ε_0 the permittivity of vacuum (8.85 × 10^{-12} N^{-1} C^2 m^{-2}), N_d the donor density, V the electrode applied potential, V_{FB} the flatband potential, and $\frac{kT}{e_0}$ is a temperature-dependent correction term. Therefore, V_{FB} can be determined from the intersection point between the extrapolated linear line and x-axis in Mott−Schottky (M-S) plots ($\frac{1}{C^2}$ versus V) and N_d can be estimated from the slope of the M-S plots according to the following equation:[1, 3]

$$N_d = \frac{2}{e_0 \varepsilon \varepsilon_0}[\frac{d\frac{1}{C^2}}{dV}]^{-1}$$

3. Calculation of Debye length

The charge carrier diffusion lengths (Debye length, L_D) for both electrodes were also calculated according to the following equation:[1, 4]

$$L_D = (\frac{\varepsilon\varepsilon_0 kT}{e^2 N_D})^{\frac{1}{2}}$$

where k is the Boltzmann constant (1.38×10^{-23} J K^{-1}) and T is the absolute temperature (K).

4. Calculation of depletion layer width

The depletion layer width (W) at 0.0 V vs. SCE can be calculated via the following equation:[1, 4]

$$W = (\frac{2\varepsilon\varepsilon_0 \phi}{eN_D})^{\frac{1}{2}}$$

where $\phi = V - V_{FB}$ $\phi = V - V_{FB}$ is the maximum potential drop in the depletion layer.

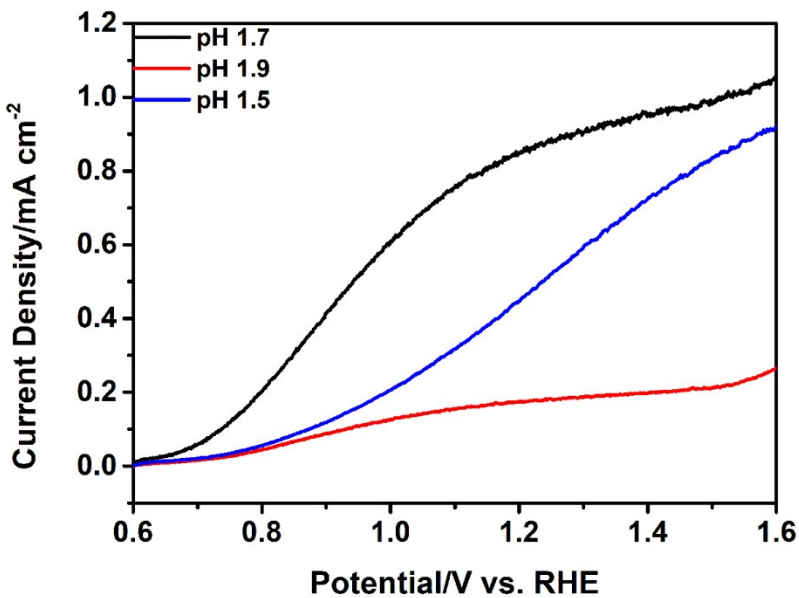

Figure S1. Linear sweep voltammograms collected from α-Fe_2O_3 synthesized at different pH under light illumination.

Figure S2. Photograph of the α-Fe_2O_3 nanostructured array synthesized at pH 1.7 and annealed at 800 ^{o}C.

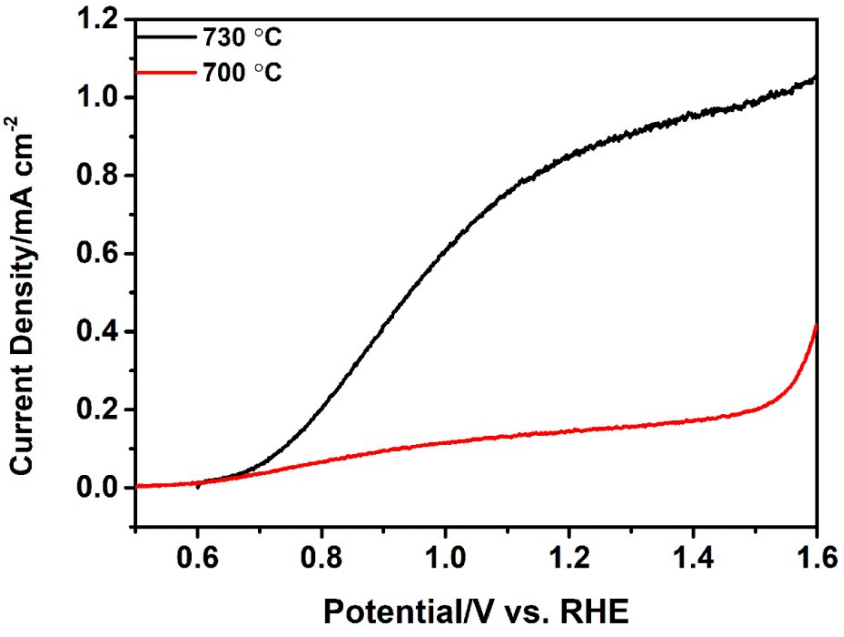

Figure S3. Linear sweep voltammograms collected from α-Fe_2O_3 nanostructured arrays synthesized at pH 1.7 and annealed at 700 ºC and 730 ºC.

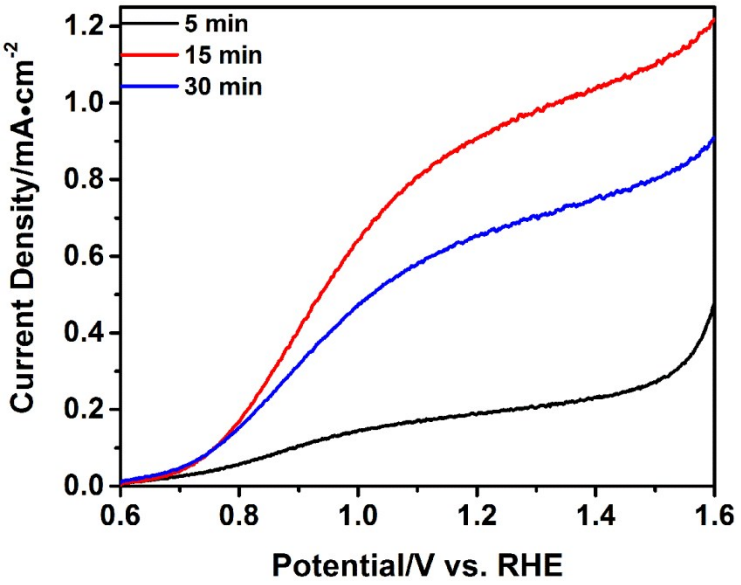

Figure S4. Linear sweep voltammograms collected from α-Fe_2O_3 nanostructured arrays synthesized at pH 1.7, annealed at 550 ºC for 1 h and at 730 ºC for different times.

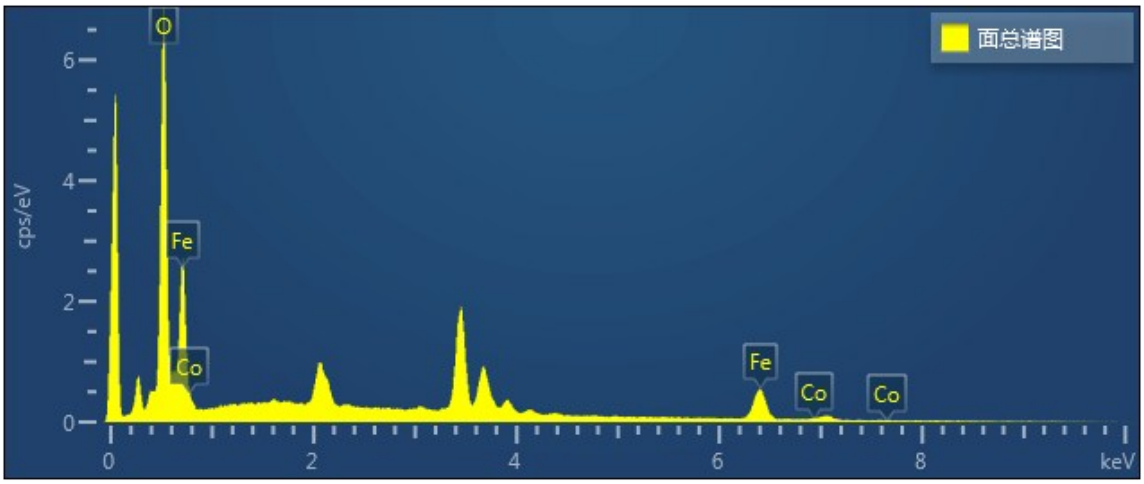

Figure S5. EDX spectrum of WN-α-Fe_2O_3@Co_3O_4.

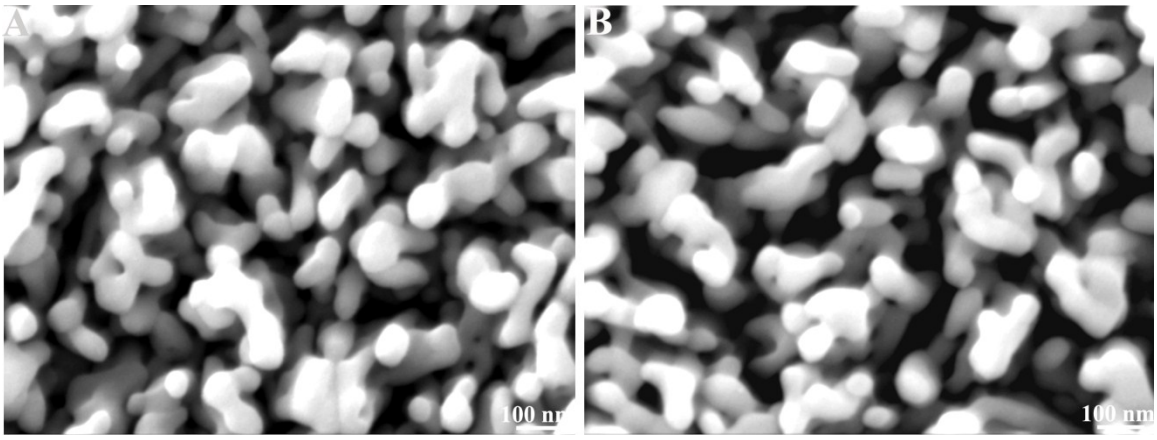

Figure S6. High-magnification FESEM image of WN-α-Fe_2O_3 before (A) and after (B) in-situ growth of Co_3O_4.

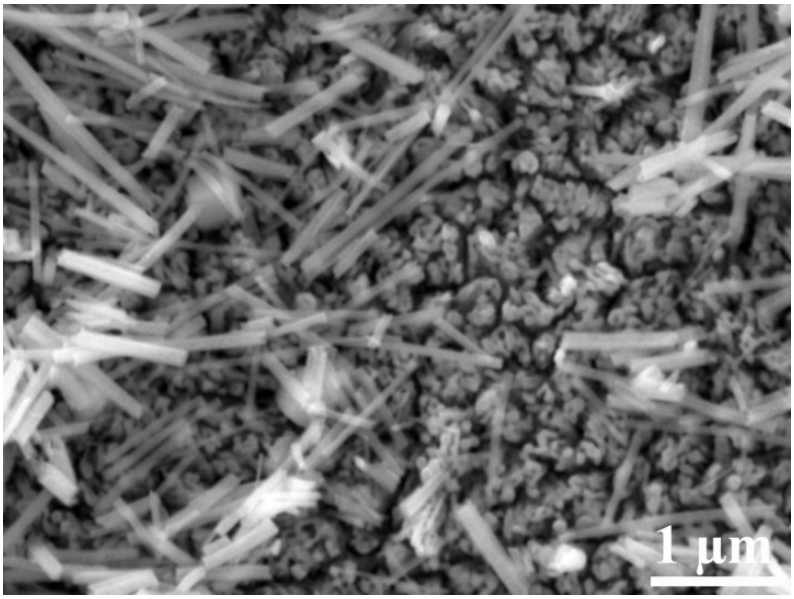

Figure S7. FESEM images of WN-α-Fe_2O_3 after growth of Co_3O_4 at reactant concentrations 1.2 times of the original ones.

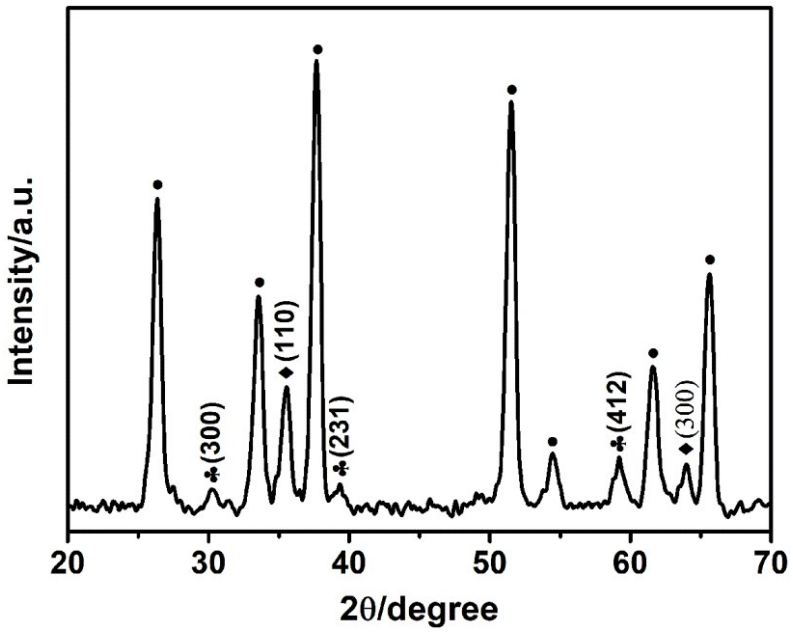

Figure S8. XRD pattern of the Co_3O_4 precursor grown on WN-α-Fe_2O_3. Except the peaks originating from FTO (marked with •) and WN-α-Fe_2O_3 (marked with ♦), the XRD pattern shows characteristic ones of cobalt-basic-carbonate phase (marked with ♣) located at 31º, 39º, and 59º, which correspond to (300), (231), and (412) planes of orthorhombic $Co(CO_3)_{0.5}(OH)\cdot 0.11H_2O$ (JCPDS card no. 048-0083).[5-6]

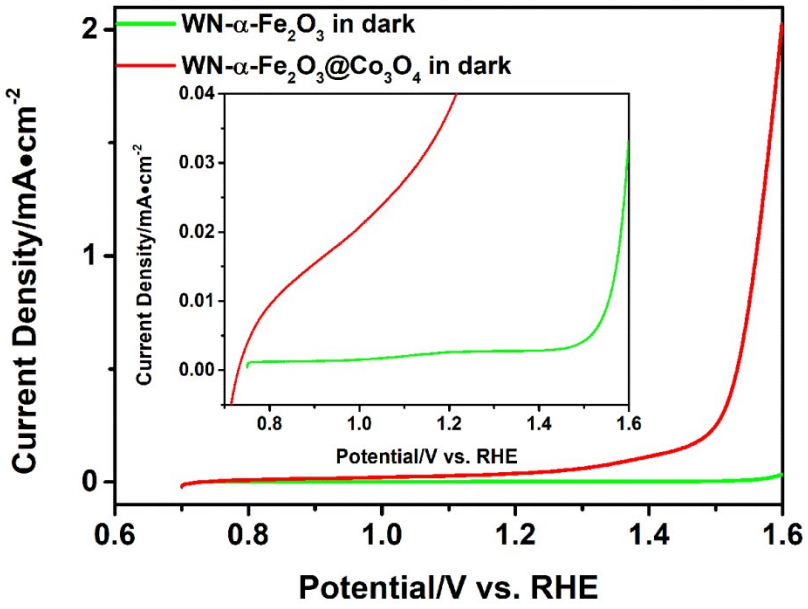

Figure S9. Enlarged linear sweep voltammograms collected from pristine WN-α-Fe_2O_3 and WN-α-Fe_2O_3@Co_3O_4 in 1 M KOH aqueous solution in dark. The inset is the curves further enlarged.

Table S1 PEC performance of representative Fe_2O_3-based photoanodes for water splitting

Photoanode	Photocurrent density (1.23 V vs. RHE)	Onset potential (V vs. RHE)	Maximum photoconversion Efficiency	Light source used	Electrolyte	Reference
CoAl-LDH/α-Fe_2O_3	2.0	0.58		AM 1.5 G, 100 mW cm^{-2}	0.1 M NaPi buffer (pH 7)	7
rGO modified 3D urchin-like α-Fe_2O_3	1.06	~0.8	0.102%	AM 1.5 G, 100 mW cm^{-2}	1 M NaOH	8
α-Fe_2O_3 with in-situ grown Co_3O_4 NPs	1.2	0.66		AM 1.5 G, 100 mW cm^{-2}	1 M NaOH	9
α-Fe_2O_3/NiOOH	0.625	0.62		AM 1.5 G, 100 mW cm^{-2}	1 M NaOH	10
α-Fe_2O_3/Co(II)/Co_3O_4	2.1 (1.53 V)	0.95		AM 1.5 and UV filter, 100 mW cm^{-2}	0.1 M KOH	11
α-Fe_2O_3@IrO_2 NPs	~3.1	0.8		KG3 filter, 100 mW cm^{-2}	1 M NaOH	12
α-Fe_2O_3 Nanowires@Co catalyst	0.54	0.77		AM 1.5 G, 100 mW cm^{-2}	1 M NaOH	13
SiO_2/α-Fe_2O_3@Co catalyst	2.7	~0.8		KG3 filter, 100 mW cm^{-2}	1 M NaOH	14
Fe_2O_3–TiO_2	2.0	0.8	0.098%	AM 1.5 G, 100 mW cm^{-2}	1 M NaOH	15
Fe-Pi/Fe_2O_3	~0.8	0.8		AM 1.5 G, 100 mW cm^{-2}	1 M NaOH	16
Sn-Fe_2O_3/CoPi	0.60	0.65		AM 1.5 G, 100 mW cm^{-2}	1M KOH	17
α-Fe_2O_3/NiCeOx	~0.62	~0.6		AM 1.5 G, 100 mW cm^{-2}	1 M NaOH	18
3D NSP@α-Fe_2O_3@CoPi	3.05	~0.7		AM 1.5 G, 100 mW cm^{-2}	1 M NaOH	19
Anodized Fe foams@Co catalyst	3.25	~0.63		AM 1.5 G, 100 mW cm^{-2}	1 M NaOH	20
CoPi/TiO_2-modified α-Fe_2O_3	~1.4	~0.68		AM 1.5 G, 100 mW cm^{-2}	1 M NaOH	21
C/Co_3O_4-Fe_2O_3	1.48	0.79	0.2%	AM 1.5 G, 100 mW cm^{-2}	1 M NaOH	22
FeOOH/Fe_2O_3	1.21	0.65		AM 1.5 G, 100 mW cm^{-2}	1 M NaOH	23
WN-α-Fe_2O_3@Co_3O_4	3.48	~0.62	0.55%	AM 1.5 G, 100 mW cm^{-2}	1 M KOH	This work

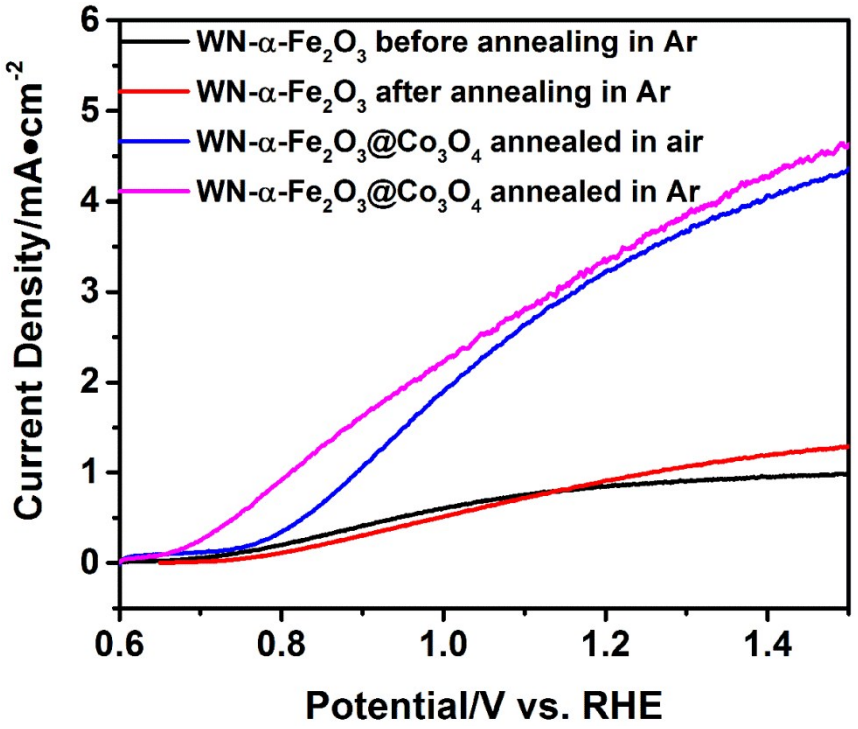

Figure S10. Linear sweep voltammograms collected from WN-α-Fe_2O_3 before and after annealing in Ar and from WN-α-Fe_2O_3@Co_3O_4 annealed in air and in Ar in 1 M KOH aqueous solution under light illumination.

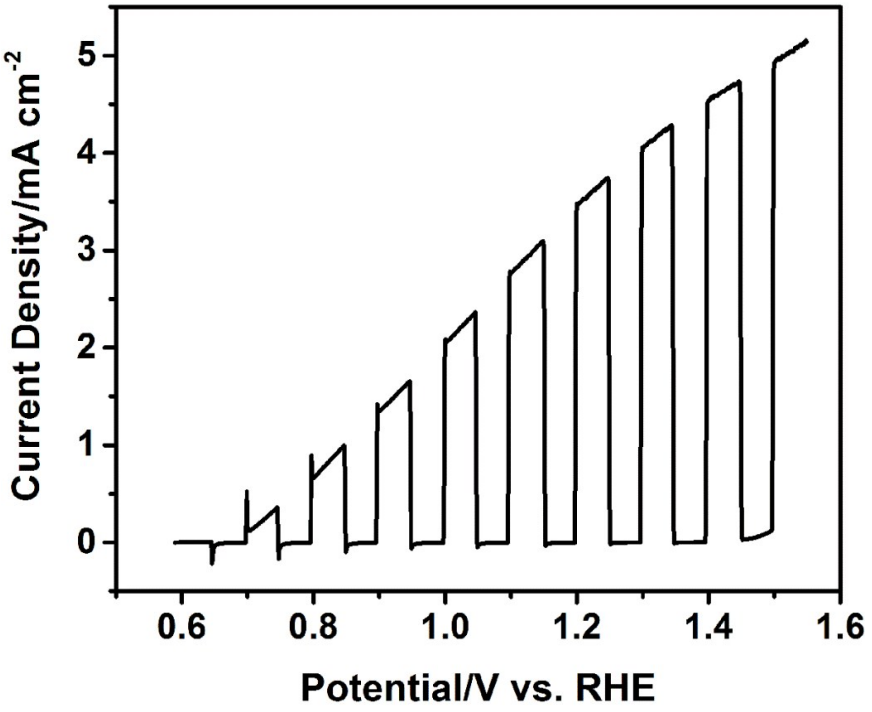

Figure S11. Linear sweep voltammograms collected from WN-α-Fe_2O_3@Co_3O_4 in 1 M KOH aqueous solution under chopped light illumination.

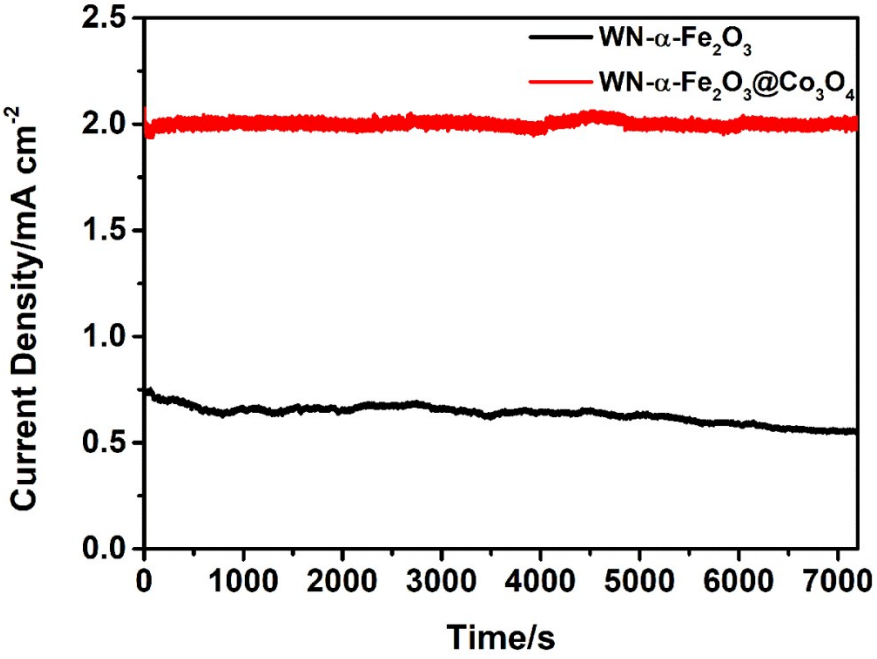

Figure S12. Photocurrent retention versus time curves of pristine WN-α-Fe_2O_3 and WN-α-Fe_2O_3@Co_3O_4 under light illumination at 1 V vs. RHE.

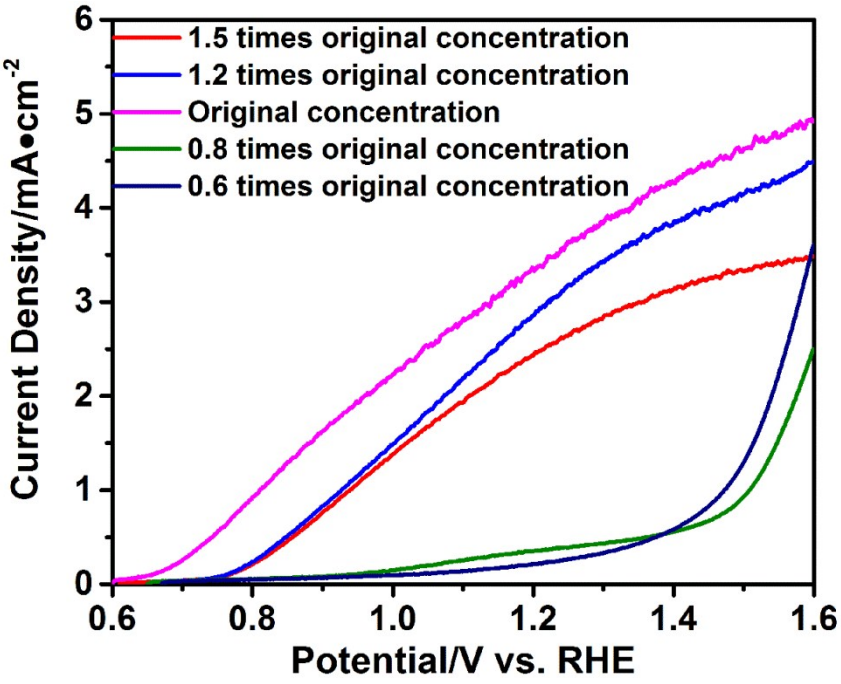

Figure S13. Linear sweep voltammograms collected from WN-α-Fe_2O_3@Co_3O_4 synthesized with different reactant concentrations in 1 M KOH aqueous solution under light illumination.

References

[1] W. Yuan, J. Yuan, J. Xie, C. M. Li, *ACS Appl. Mater. Interfaces,* 2016, **8**, 6082.

[2] Z. Li, W. Luo, M. Zhang, J. Feng, Z. Zou, *Energy Environ. Sci.,* 2013, **6**, 347.

[3] K. Gelderman, L. Lee, S. W. Donne, *J. Chem. Educ.*, 2007, **84**, 685.

[4] C. Fàbrega, D. Monllor-Satoca, S. Ampudia, A. Parra, T. Andreu, J. R. Morante, *J. Phys. Chem. C,* 2013, **117**, 20517.

[5] R. Xu, H. C. Zeng, *J. Phys. Chem. B,* 2003, **107**, 12643.

[6] L. Li, M. Liu, S. He, W. Chen, *Anal. Chem.*, 2014, **86**, 7996.

[7] R. Chong, B. Wang, C. Su, D. Li, L. Mao, Z. Chang and L. Zhang, *J. Mater. Chem. A.*, 2017, **5**, 8583.

[8] A. G. Tamirat, W.-N. Su, A. A. Dubale, C.-J. Pan, H.-M. Chen, D. W. Ayele, J.-F. Lee and B.-J. Hwang, *J. Power Sources*, 2015, **287**, 119.

[9] L. Xi, P. D. Tran, S. Y. Chiam, P. S. Bassi, W. F. Mak, H. K. Mulmudi, S. K. Batabyal, J. Barber, J. S. C. Loo and L. H. Wong, *J. Phys. Chem. C.*, 2012, **116**, 13884.

[10] F. Malara, A. Minguzzi, M. Marelli, S. Morandi, R. Psaro, V. Dal Santo and A. Naldoni, *ACS Catalysis*, 2015, **5**, 5292.

[11] S. C. Riha, B. M. Klahr, E. C. Tyo, S. Seifert, S. Vajda, M. J. Pellin, T. W. Hamann and A. B. F. Martinson, *ACS nano*, 2013, **7**, 2396.

[12] T. S. David, C. Maurin, S. Kevin and G. Michael, *Angew. Chem. Int. Edit.*, 2010, **49**, 6405.

[13] L. Li, Y. Yu, F. Meng, Y. Tan, R. J. Hamers and S. Jin, *Nano Lett.*, 2012, **12**, 724.

[14] A. Kay, I. Cesar and M. Grätzel, *J. Am. Chem. Soc.*, 2006, **128**, 15714.

[15] B. Davide, C. Giorgio, G. Alberto, M. Chiara, W. M. E. A., K. Kimmo, S. Cinzia, T. Stuart, G. Yakup, R. Tero-Petri, B. Laura, B. Elza, V. T. Gustaaf, L. Helge and M. Sanjay, *Adv. Mater. Interfaces*, 2015, **2**, 1500313.

[16] Z. Hu, Z. Shen and J. C. Yu, *Chem. Mater.*, 2016, **28**, 564.

[17] W. Jian, S. Jinzhan and G. Liejin, *Chem– Asian J.*, 2016, **11**, 2328.

[18] H. Lim, J. Y. Kim, E. J. Evans, A. Rai, J.-H. Kim, B. R. Wygant and C. B. Mullins, *ACS Appl. Mater. Interfaces*, 2017, **9**, 30654.

[19] Y. Qiu, S.-F. Leung, Q. Zhang, B. Hua, Q. Lin, Z. Wei, K.-H. Tsui, Y. Zhang, S. Yang and Z. Fan, *Nano Lett.*, 2014, **14**, 2123.

[20] K. J. Soo, N. Yoonsook, K. Jin, C. Hyelim, J. T. Hwa, A. Docheon, K. Jae-Yup, Y. Seung-Ho, P. Hyeji, Y. Jun-Ho, C. Wonyong, D. D. C., C. Heeman and S. Yung-Eun, *Angew. Chem. Int. Ed.*, 2017, **56**, 6583.

[21] M. G. Ahmed, I. E. Kretschmer, T. A. Kandiel, A. Y. Ahmed, F. A. Rashwan and D. W. Bahnemann, *ACS Appl. Mater. Interfaces*, 2015, **7**, 24053.

[22] P. Zhang, T. Wang, X. Chang, L. Zhang and J. Gong, *Angew. Chem. Int. Edit.*, 2016, **55**, 5851.

[23] K. J. Young, Y. D. Hyun, K. Kyoungwoong and L. J. Sung, *Angew. Chem. Int. Ed.*, 2016, **55**, 10854.